Available online at www.sciencedirect.com
SCIENCE DIRECT®
Composites Science and Technology 65 (2005) 129–136
COMPOSITES SCIENCE AND TECHNOLOGY
www.elsevier.com/locate/compscitech

Effect of surface treatment on the hydrolytic stability of E-glass fiber bundle tensile strength

E.N. Brown *, A.K. Davis [1], K.D. Jonnalagadda [2], N.R. Sottos

Department of Theoretical and Applied Mechanics, University of Illinois at Urbana-Champaign, 216 Talbot Lab, 104 S. Wright Street, Urbana, IL 61801, USA

Received 17 February 2004; received in revised form 11 June 2004; accepted 1 July 2004
Available online 25 August 2004

Abstract

The tensile strength of glass fiber bundles is highly dependent on flaw nucleation and growth from contact abrasion and hydrolytic degradation. The effect of fiber surface treatment on the hydrolytic stability of tensile strength is investigated for E-glass fiber bundles with four commercial sizings. Acoustic emission (AE) generated by individual fiber fracture events provides a means to determine a Weibull distribution of fiber strengths. Fiber bundles with starch, starch and silane, starch and wax, and epoxy surface treatments are tested following exposure to 10%, 40%, 80% relative humidity and immersion in water. The tensile break strength, number of breaks at peak load, and Weibull moduli of the glass fiber bundles are strongly dependent on the humidity level. The different surface treatments considered in this investigation strongly alter the absolute mechanical properties and the effect of exposure to humidity.

Keywords: A. Glass fibers; A. Coating; C. Failure criterion; D. Acoustic emission; Weibull distribution

1. Introduction

Glass fiber is the reinforcement component in a wide variety of composite applications ranging from aircraft and automobiles to printed wire circuit board substrates and sporting goods. While an ultimate stress of 3.5 GPa has been measured in small diameter glass fibers [1], flaws resulting from contact abrasion and hydrolytic degradation significantly reduce the realizable strength of commercial fibers used for manufacturing [2]. Moisture interaction with the metal oxides in E-glass leads to corrosion-induced defects and decreased fiber mechanical strength [3]. During the manufacturing process a surface treatment, referred to as a sizing, is applied to protect the fibers and to improve wettability of the fiber surfaces by liquid resin.

Sizing generally consists of a water-based mixture containing a lubricant, a film former, and a coupling agent applied from an aqueous emulsion (e.g. epoxy, poly(vinly acetate), etc.) or a solution [4]. An extensive study of the effect of surface treatment, fiber diameter, gage length, and strain rate on glass fiber bundles [5–8] reported an increase in bundle strength, of as much as 90%, associated with several surface treatments. The increase in strength is attributed to the sizing protecting glass fibers from contact abrasion and improving load transfer between fibers. Studies of the hydrolytic effects on single filaments [9] and bundles [10] have shown sizing can dramatically reduce the rate of humidity aging

* Corresponding author. Present address: Materials Science and Technology Divison, MS-E544, Los Alamos National Laboratory, Los Alamos, NM 87544, USA. Tel.: +1 505 667 0799; fax: +1 505 667 2185.
E-mail address: en_brown@lanl.gov (E.N. Brown).
[1] Present address: Honeywell Engine Division, Phoenix, AZ 85034, USA.
[2] Present address: Motorola Advanced Technology Center, 1301 E. Algonquin Road, Schaumburg, IL 60196, USA.

0266-3538/$ - see front matter © 2004 Elsevier Ltd. All rights reserved.
doi:10.1016/j.compscitech.2004.07.001

and the associated drop in glass fiber strength. The hydrolytic degradation of glass fiber reinforced polymer composites with [11] and without [12–14] the effect of sizing has also been studied.

This paper investigated the relationship between surface treatment and hydrolytic damage on E-glass fiber failure. E-glass fiber bundles consisted of 204 individual G150-type, 9 μm nominal diameter filaments [15]. Four types of surface treatment types are explored: Type I with starch, Type II with starch and silane, Type III with starch and wax, and Type IV with epoxy. Silane added to the starch chemistry in the Type II bundles is intended to protect the glass against hydrolytic damage. Wax added to the starch chemistry in the Type III bundles is proposed to reduce damage caused by frictional sliding between fibers. Epoxy sizing in the Type IV bundles is applied to enhance interfacial adhesion between the fiber bundle and an epoxy matrix.

Failure stress and Weibull parameters are measured at four humidity levels: 10%, 40%, 80% relative humidity (RH) and immersion in water. Previous measurements of fiber strength frequently employed single-filament tests [16], fractography [17], load drop [18], and strain measurements [19]. These methods are limited to a single fiber or a small bundle and estimate the characteristic flaw distribution of a fiber bundle. Weibull modulus values for glass fibers reportedly range from 3–15 at ambient laboratory humidity levels [20–22]. In the present investigation, an acoustic emission (AE) technique is applied to test a complete fiber bundle during tensile loading. When a fiber under applied stress fractures, a portion of the elastic energy is consumed in creating the new fracture surface and the remainder is radiated in the form of stress waves. Each fiber break in a bundle is uniquely detected by recording AE during fracture [23].

2. Overview of fiber bundle failure

When a glass fiber bundle fails, it is common for the individual filaments to fail over a wide range of loads. Many weak fibers fail at low loads, redistributing the applied load onto the stronger fibers. This type of failure mechanism cannot be accurately described by a single average strength value. While ''weakest link'' methods have been presented in the literature [24–26], a different model must be adopted to capture the distribution of strengths found when testing fiber bundles.

Coleman [27] first suggested that the probability of fiber failure follows the form of a Weibull [28] distribution. He considered a fiber of non-dimensional length L containing one or more critical flaws, where $L = 1$ is the minimum distance between two flaws on a single fiber below which the flaws interact. The only flaw that is considered to influence failure is the flaw of lowest failure stress, which becomes the failure stress of the fiber σ_f. The probability that an individual fiber will fail at a given stress level can be written as

$$P_f(\sigma_f) = 1 - \exp\left[-L\left(\frac{\sigma_f}{\sigma_0}\right)^{\beta}\right]. \quad (1)$$

Cowking et al. [23] proposed a model applying a Weibull distribution to characterize a fiber bundle in the form

$$\frac{N(\sigma_f)}{N_0} = \exp\left[-\left(\frac{\sigma_f}{\sigma_0}\right)^{\beta}\right], \quad (2)$$

where N is the number of unfractured fibers corresponding to a stress in each fiber of σ_f and N_0 is the number of fibers in a bundle. The Weibull modulus β and the scale factor σ_0 are to be determined. The stress for the ith fiber break is calculated assuming the applied load F is equally shared among the N similar fibers surviving before the break, thus

$$\sigma_i = \frac{F}{NA} = \frac{F}{(N_0 - (i-1))\pi r_f^2}, \quad (3)$$

where N is the total number of fibers in the bundle and r_f is the radius of the fiber. Taking the natural logarithm of Eq. (2) twice and manipulation yields

$$\beta \ln \sigma_f + \beta \ln \sigma_0 = \ln \ln \left(\frac{N_0}{N(\sigma_f)}\right). \quad (4)$$

From the bundle test data, a plot of $\ln\ln(N_0/N)$ against $\ln(\sigma)$ is anticipated to give a straight line with slope β, the Weibull modulus. The Weibull analysis assumes that the material is statistically homogeneous throughout its length, the stress–strain relationship for a single fiber is linear elastic up to fracture, the applied load is uniformly distributed among the surviving fibers, and the interactions between fibers resulting from friction and twisting are negligible.

3. Materials and method

3.1. Sample preparation

A typical sample for tensile testing is shown in Fig. 1. Samples were fabricated by cutting six-inch lengths of fiber directly from bobbins supplied by Advanced Glass Fiber Yarns (AGY). Before being wound onto the bobbins, 0.7 turns per inch of twist was placed in the bundles by the manufacturer. The effect of twist has been discussed by Davis [29]. For this investigation the twist was removed prior to making the samples by suspending the cut bundle from one end with a small weight on the free end of the bundle. The hanging bundles were placed under a hood to prevent movement due to air circulation and allowed to oscillate until all of the twist was re-

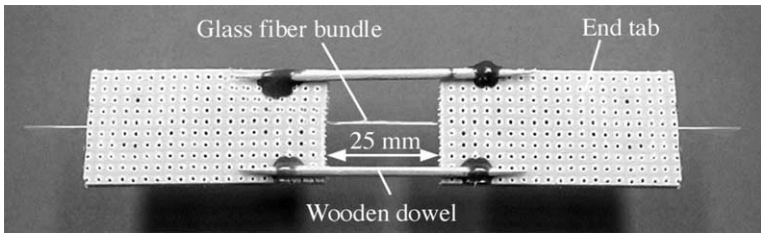

Fig. 1. Glass fiber bundle tensile specimen.

moved. The amount of force on the fiber from the weight was approximately 0.8 N, which was a low enough load that no fiber breaks occurred. A 25 mm gage length of fibers was chosen because of the lower variation of strength found in shorter samples [5].

Silicone rubber molds were made to position the end tabs and ensure that gage length was 25 mm. End tabs (25 mm × 50 mm) were cut from perforated fiberglass circuit boards. Two tabs were placed in the mold, and coated with a highly viscous epoxy. Untwisted bundles were then laid across the mold, and kept under a uniform tension with small weights on the bundle ends. Two more tabs were placed on top of the bottom tabs, sandwiching the bundle between them. In addition to providing a practical method of mounting fiber bundles in the grips of an Instron testing machine, the end tabs also served as a wave-guide to transmit acoustic waves from the glass fibers to the piezoelectric sensor [20]. Two small wooden dowels were glued to the end tabs as shown in Fig. 1 to maintain a consistent gage length and protect the fibers from damage prior to testing. After a 24-h cure, the specimens were placed into an oven or humidity chamber. Care was taken not to touch the bundle gage length during manufacturing and testing to prevent damage to the fibers, which would shift the distribution of fiber breaks.

3.2. Environmental conditioning

A Plexiglass chamber was constructed to achieve different humidity levels. Low RH values (10%, 40%) were obtained with a vacuum pump that pumped air out of the chamber through a desiccant column (Anhydrous $CaSO_4$, W.A. Hammond Drierite Co.) and then back into the chamber. A timer was used to maintain the desired humidity level. The higher, 80% RH environment was created in the chamber using a modified warm-air room humidifier. A dial setting on the humidifier was used to maintain the desired humidity level. The immersion condition was obtained by soaking the fiber bundles in distilled water for 24 h. Distilled water was used to prevent drops in strength associated with salts [30]. In all cases samples were placed in the environmental chamber until a steady desired humidity level was attained and stored in the environmental chamber until testing.

3.3. Experimental apparatus

E-glass fiber bundles were loaded in tension using an Instron Mini 44 load frame with a 500 N (full scale) load cell. Individual fiber breaks during the bundle test were detected with an AE technique [23]. Load–strain data and AE–time data were acquired concurrently by computer control, ensuring accurate correspondence of the AE data representing individual fiber failure events with the load–strain data, shown schematically in Fig. 2. The load frame and load–strain data acquisition were controlled by Labview software via an IEEE bus connection. Energy released during fiber fracture were detected with a 150 kHz piezoelectric AE sensor and preamplifier (DECI SE 150-M, Dunegan and DECI 400p-20H, Dunegan). The sensor was attached to the lower end tab using a clamp to reduce interface loss. A 400 MHz oscilloscope (9310AM, LeCroy) recorded an amplified signal from the sensor, providing the occurrence times of 205 signals: one initializing signal followed by 204 fiber failures. The threshold voltage to trigger the oscilloscope was 0.5 V. As the number of recorded acoustic events never exceeds 205, it is concluded that all of the AE events recorded after triggering represent fiber fracture. Upon completion of the test, fiber break data were transferred to a computer via an RS232 connection.

Specimens were mounted into the test frame directly from the environmental chamber. To ensure the fibers

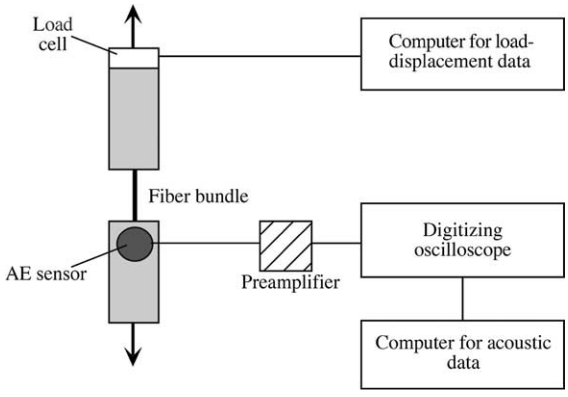

Fig. 2. Schematic of the experimental setup for testing glass fiber bundles with the AE technique.

were not shock loaded, a small compressive load was applied on the sample while the dowels were cut. The crosshead was zeroed with 1 N applied to the fiber bundle. Bundles were tested with a constant displacement rate of 50 μm/min until all fibers were broken. The displacement rate was chosen to maximize the accuracy to AE data acquisition [20] and reduce strain rate effects associated with glass fiber failure [6,31]. Average values and standard deviations of peak load, fiber breaks at peak load, stain at failure, and Weibull modulus were calculated from 20 specimens for each combination of sizing type and humidity level.

3.4. Analysis

Nominal strain values were calculated directly from the gage length and cross head displacement. Fig. 3 shows typical load–strain data for a fiber bundle along with the individual fiber breaks as detected by the AE sensor. Excluding a small nonlinear region due to machine and fixture compliance, the load–strain curve is linear until the first fiber break. The load continues to increase until reaching a critical point, followed by rapid failure. The peak load, strain to failure, and number of breaks to peak load are recorded.

The stress in the surviving fibers after each break is calculated by Eq. (3). A Weibull plot is created by plotting $\ln(\sigma)$ versus the $\ln\ln(N_0/N)$, shown in Fig. 4, from which the Weibull modulus β is extracted. For values of $\ln\ln(N_0/N)$ above a critical point, indicated by a line in Fig. 4, the data become highly nonlinear. The data above this line are excluded from calculation of the slope. Failure of the final fibers likely deviates from the Weibull model for a combination of reasons. Load sharing between broken fibers from surface forces takes on an increased significance compared with the load carrying ability of individual fibers. Breaking fibers can cause damage to the surface of load bearing fibers during recoil, creating stress concentrations and premature failure in adjacent fibers. Moreover, measurement of the low total loads carried by the few remaining fibers prior to failure is limited by the sensitivity of the load cell.

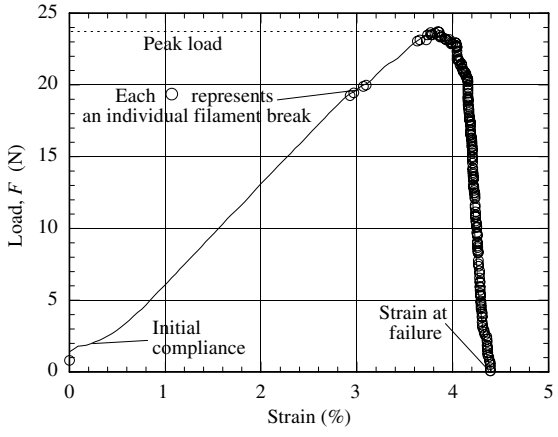

Fig. 3. Representative load–strain relationship for fiber bundles [Type II E-glass fiber bundle at 100% RH]. The continuous load–strain data set is given by the smooth continuous curve, the failure load and strain of each individual fiber is indicated by a circle (○).

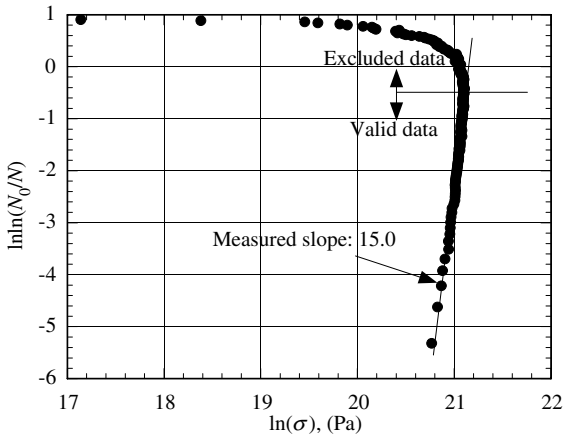

Fig. 4. Representative Weibull plot for fiber bundle failure [Type II E-glass fiber bundle at 100% RH].

4. Results and discussion

The four types of fiber bundles (I, II, III, IV) were tested after conditioning in four different levels of humidity: 10, 40, 80 RH and immersion in water. Twenty samples were tested for each combination of surface treatment and humidity level, and the average and standard deviation of each data set were calculated, as listed in Tables 1–4. The data for the different surface treatments were compared at each humidity level. Representative load–strain curves at each humidity level are plotted for the individual fiber bundle types in Figs. 5–8.

The average peak load for each type of fiber bundle and humidity level are summarized in Table 1. Prior to reaching peak load, individual fibers fail and their load is redistributed to neighboring fibers while the bundle remains intact. Following peak load, redistribution of the applied load exceeds the critical stress of the remaining fibers, leading to a rapid-cascading failure of the bundle. For the displacement-control case investi-

Table 1
Effect of relative humidity on averages and standard deviations of peak load for fiber bundles with different sizing types

Relative humidity (%)	Type I	Type II	Type III	Type IV
10	19 ± 1	24 ± 2	22 ± 1	17 ± 2
40	18 ± 2	23 ± 2	21 ± 1	18 ± 4
80	19 ± 2	24 ± 1	22 ± 2	17 ± 1
100	16 ± 1	21 ± 2	16 ± 2	17 ± 2

Table 2
Effect of relative humidity on averages and standard deviations of the number of breaks at peak load for fiber bundles with different sizing types

Relative humidity (%)	Type I	Type II	Type III	Type IV
10	11 ± 4	8 ± 3	12 ± 5	11 ± 3
40	13 ± 5	8 ± 4	20 ± 8	7 ± 3
80	15 ± 6	9 ± 4	14 ± 6	10 ± 4
100	21 ± 5	9 ± 4	17 ± 5	5 ± 2

Table 3
Effect of relative humidity on averages and standard deviations of the Weibull modulus for fiber bundles with different sizing types

Relative humidity (%)	Type I	Type II	Type III	Type IV
10	14 ± 4	11 ± 3	5 ± 2	13 ± 2
40	7 ± 2	7 ± 2	4 ± 1	14 ± 5
80	9 ± 3	15 ± 6	6 ± 2	14 ± 4
100	9 ± 3	17 ± 7	8 ± 4	17 ± 7

Table 4
Effect of relative humidity on averages and standard deviations of strain at failure for fiber bundles with different sizing types

Relative humidity (%)	Type I	Type II	Type III	Type IV
10	3.6 ± 0.3	4.1 ± 0.3	3.9 ± 0.3	3.1 ± 0.3
40	3.2 ± 0.3	3.5 ± 0.3	3.7 ± 0.3	3.0 ± 0.3
80	4.2 ± 0.5	4.5 ± 0.3	4.2 ± 0.6	3.1 ± 0.1
100	3.8 ± 0.4	3.8 ± 0.3	3.9 ± 0.5	2.9 ± 0.3

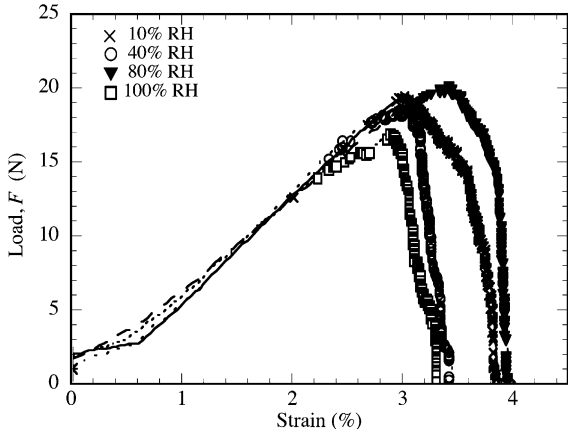

Fig. 5. Representative load–strain data for Type I fiber bundles at each humidity level.

gated in this work, the load continues to drop from the peak value as subsequent fibers fail.

The peak load for Types I, II and III fiber bundles treated with starch-based sizings followed similar dependence on humidity level, as shown in Fig. 9. All three were statistically independent of the humidity level for the non-saturated cases. For bundles immersed in water, however, the peak load decreased significantly. Of the starch-based sizings, the Type II bundles with silane displayed the largest peak load of all the sizing types and the least drop in peak load following immersion. The Type III bundles with wax displayed a peak load greater than the bundles with only starch Type I.

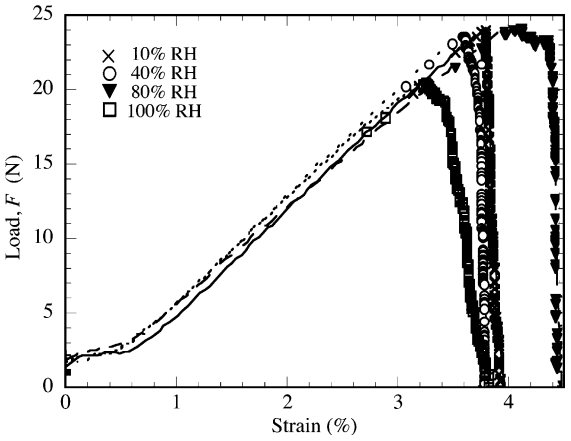

Fig. 6. Representative load–strain data for Type II fiber bundles at each humidity level.

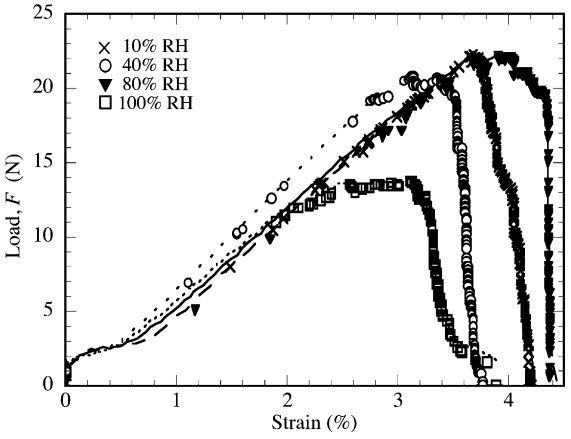

Fig. 7. Representative load–strain data for Type III fiber bundles at each humidity level.

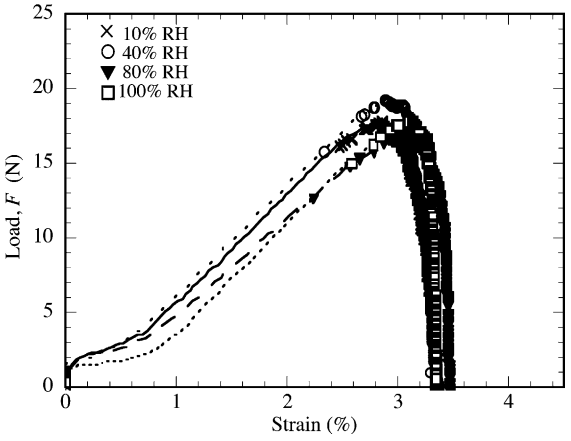

Fig. 8. Representative load–strain data for Type IV fiber bundles at each humidity level.

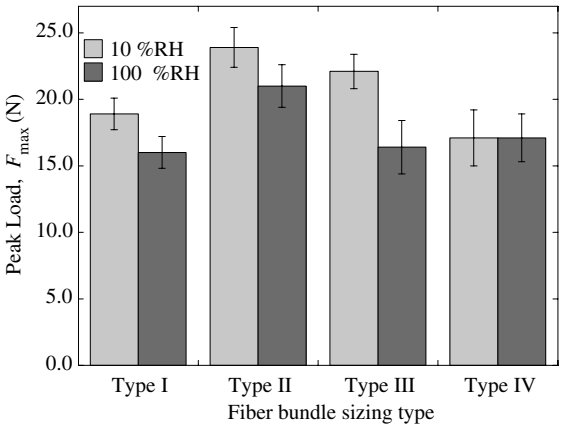

Fig. 9. Effect of relative humidity on peak load for fiber bundles with different sizing types. The error bars represent ±;1 SD.

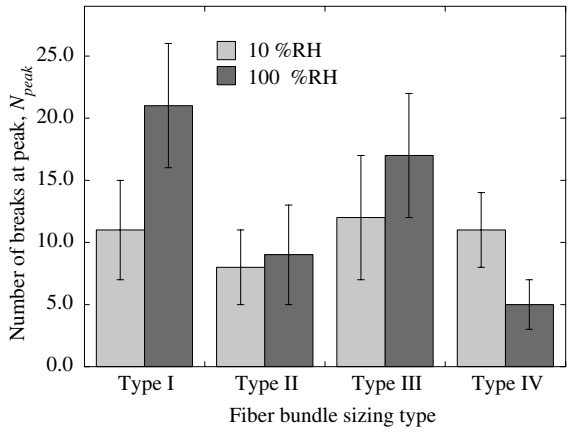

Fig. 10. Effect of relative humidity on the number of breaks at peak load for fiber bundles with different sizing types. The error bars represent ±1 SD.

Following immersion the peak loads of Type III and Type I bundles were indistinguishable. The peak load of fiber Type IV bundles with the epoxy sizing was independent of the humidity level, including saturation. Moreover, the peak load was statistically equivalent to the saturated bundles with Type III and Type I sizing types.

The Type IV fibers used in this investigation were part of a small study batch made specifically for this project. All other fiber samples were taken from large production runs. As indicated by Fig. 9, the strength of the type IV bundles is lower than expected for an epoxy size. After a series of independent tensile tests by the manufacturer, we concluded that the reduction in strength could be attributed to the small production run.

A summary of the number of fiber breaks prior to peak load for each fiber type and humidity level is listed in Table 2. All fiber bundles with starch-based sizings (with the exception of Type III bundles at 40% RH) exhibited a general trend of increasing number of breaks prior to peak load with increasing humidity level, as shown in Fig. 10. Fiber bundles with Type I and Type III sizings exhibited a similar number of breaks and large dependence on humidity, indicative of a large number of fibers experiencing hydrolytic damage. Fiber bundles with Type II sizing exhibited less breaks and minimal dependence on humidity. Fiber bundles with Type IV sizing exhibited a number of breaks similar to the Type II sizing, but had a marked decrease in the number of breaks with increasing humidity, indicating reduced hydrolytic degradation. Fibers broken prior to peak load are weak or damaged fibers; a larger number of breaks denotes a larger number of fibers with a critical stress value significantly below the mean.

Table 3 lists the Weibull moduli of the fiber bundle types. The Weibull modulus indicates the distribution of critical stress values for the fibers in a bundle. Larger Weibull modulus values represent a lower variance of the distribution relative to the mean, and hence, a less flaw dependent material. All the fiber bundles with starch-based sizings exhibited a decrease of Weibull modulus from 10% to 40% RH followed by an increase of Weibull modulus with increasing humidity level. The largest Weibull modulus for fiber bundles with Type I sizing was at 10% RH; the largest Weibull modulus for fiber bundles with Type II and Type III sizing types was following immersion. Fiber bundles with Type III sizing exhibited the lowest Weibull modulus of the four sizing types for the full range of humidity levels investigated. Type IV fiber bundles with epoxy sizing exhibited the highest values of Weibull modulus, which increased with increasing humidity. Measured Weibull modulus valued for 10% to 80% RH corresponds to the range of Weibull modulus values given in the literature [20–22]. Following immersion the Weibull modulus values increase above previously reported values.

The nominal strain at failure, listed in Table 4, measures the elongation of the last fibers in the bundle to break. As shown in Figs. 5–7, the strain to failure of fiber bundles with starch sizes (Types I, II, and III) is dependent on humidity level. Moreover, the samples with low strain to failure exhibited either a reduced strain corresponding to the peak load or a more rapid-cascading failure of the individual fibers following peak load. The strain at peak load is closely correlated to the peak load and the narrower distribution of fiber failures is described by lower values of the Weibull modulus. Therefore, fiber bundles with a starch size exposed to immersion in water and 40% RH had low strain to failure corresponding to the humidity levels with lowest peak load and lowest Weibull modulus, respectively. The strain to failure of fiber bundles with epoxy size is independent of humidity level, as shown in Fig. 8. Fiber bundles with

the starch-based sizing types exhibited strain at failure values between 3.5% and 4.5%, while fiber bundles with the epoxy-based sizing exhibited strain at failure values of approximately 3.0%.

5. Conclusions

The effect of four surface treatments – starch (Type I), starch and silane (Type II), starch and wax (Type III), and epoxy (Type IV) – on the hydrolytic stability of E-glass fiber bundles was investigated. Acoustic Emission (AE) monitoring provided a load history of bundle failure, which was used to evaluate the number of failures at peak load and the Weibull modulus.The type of surface treatment on a glass fiber affected both the failure strength and the dependence on humidity level. Moreover, fiber bundles with the starch-based sizings exhibited similar trends in humidity dependence, which were uniquely different from trends of fibers with the epoxy-based sizing.

The number of breaks at failure and Weibull moduli were both strongly dependent on humidity level. Fibers with starch sizing (Type I) and starch and wax sizing (Type III) both had an increasing number of breaks with increasing humidity, fibers with starch and silane sizing (Type II) had a lower number of breaks and nominal dependence on humidity. Fibers with epoxy sizing (Type IV) had a low number of breaks, which decreased with increasing humidity. All fiber bundles with starch-based sizings exhibited a decrease of Weibull modulus from 10% to 40% RH followed by an increase of Weibull modulus, while the fibers with epoxy sizing (Type IV) had an increase of Weibull modulus over the full range of humidity.

Below saturation, the peak load was independent of humidity but was strongly dependent on surface treatment. The average non-saturated peak loads were 24, 22, 19, and 17 N for the Type II, Type III, Type I, and Type IV bundle types, respectively. At saturation, fiber bundles with the starch-based sizings exhibited a decrease in peak load. The peak load of fiber bundles with starch sizing (Type I) and starch and wax sizing (Type III) decreased to that of the weakest fibers (Type IV).

Acknowledgments

The authors gratefully acknowledge Advanced Glass Fiber Yarns (AGY) for providing financial support and the glass fibers used in this research and thank Doug Lyle of AGY for technical support and helpful discussions. Any opinions, findings, and conclusions or recommendations expressed in this publication are those of the authors and do not necessarily reflect the views of AGY. Mechanical testing was performed in the Advanced Materials Testing Lab (AMTEL) of the University of Illinois at Urbana-Champaign with the assistance of Dr. P. Kurath.

References

[1] Griffith AA. The phenomena of rupture and flow in solids. Philos Trans R Soc Lond A 1920;221:163–98.
[2] Spaude R. Corrosion phenomena in glass fibers and glass fiber reinforced polymers. Int J Mater Product Technol 1987;2:247–57.
[3] Schutte CL. Environmental durability of glass-fiber composites. Mater Sci Eng Rep 1994;13(7):265–323.
[4] Jones FR. Interphase formation and control in fibre composite materials. Key Eng Mater 1996;116:41–60.
[5] Thomas WF. An investigation of the factors affecting the strength of glass fiber strand. Glass Technol 1971;12(3):60–4.
[6] Thomas WF. An investigation of the factors affecting the strength of glass fiber strand. Part 2. Glass Technol 1972;13(1):17–21.
[7] Thomas WF. An investigation of the factors affecting the strength of glass fiber strand. The strength in polyester resin. Glass Technol 1972;13(4):122–5.
[8] Thomas WF. An investigation of the factors affecting the strength of glass fiber strand. Part 4. The effect of fiber surface area. Glass Technol 1972;13(5):141–4.
[9] DiBenedetto AT, Lex PJ. Evaluation of surface treatments for glass fibers in composite materials. Polym Eng Sci 1989; 29(8):543–55.
[10] Cameron NM. The effect of environment and temperature on the strength of E-glass fibres. Part 2. Heating and ageing. Glass Technol 1968;9(5):121–30.
[11] Barraza HJ, Aktas L, Hamidi YK, Long Jr J, O'Rear EA, Altan MC. Moisture absorption and wet-adhesive properties of resin transfer molded (RTM) composites containing elastomer-coated glass fibers. J Adhesion Sci Technol 2003;17(2):217–42.
[12] Viña J, Castrillo MA, Argüelles A, Viña I. Effects of natural and accelerated aging on the static and dynamic behavior of glass-fiber-reinforced polyetherimide. J Mater Sci Lett B 1998; 17(20):1711–3.
[13] Kaushal S, Tankala K, Rao R, Kishore. Some hygrothermal effects on the mechanical-behavior and fractography of glass-epoxy composites with modified interface. J Mater Sci 1991;26(23):6293–9.
[14] Jensen RE, Johnson CE, Ward TC. Investigation of a waterborne epoxy for E-glass composites. J Polym Sci B 2000; 38(18):2351–565.
[15] Owens-Corning Corp. Product literature. Owens-Corning Technical Report, March; 1983.
[16] ASTM 3379. Standard test method for tensile strength and Young's modulus for high-modulus single-filament materials; 1982.
[17] Mecholsky JJ, Rice RW, Freiman SW. Prediction of fracture energy and flaw size in glasses from measurements of mirror size. J Am Ceram Soc 1974;57(10):440–5.
[18] Fuwa M, Bunsell AR, Harris B. An evaluation of acoustic emission techniques applied to carbon fiber composites. J Appl Phys D 1976;9(2):353–64.
[19] Chi ZF, Chou TW, Shen GY. Determination of single fibre strength distribution from fibre bundle testings. J Mater Sci 1984;19(10):3319–24.
[20] Sha JH, Siddiqui AM, Sweet MAS. Fracture strength of E-glass fibre strands using acoustic emission. NDT&E Int 1997; 30(6):383–8.

[21] Gurvich MR, DiBenedetto AT, Pegoretti A. Evaluation of the statistical parameters of a Weibull distribution. J Mater Sci 1997;32(14):3711–6.
[22] Zinck P, Pays MF, Rezakhanlou R, Gerard JF. Mechanical characterization of glass fibres as an indirect analysis of the effect of surface treatment. J Mater Sci 1999;34(9):2121–33.
[23] Cowking A, Attou A, Siddiqui AM, Sweet MAS, Hill R. Testing E-glass fiber bundles using acoustic-emission. J Mater Sci 1991;26(5):1301–10.
[24] Hui CY, Phoenix SL, Shia D. The single-filament-composite test: a new statistical theory for estimating the interfacial shear strength and Weibull parameters for fiber strength. Compos Sci Technol 1997;57(12):1707–25.
[25] Yavin B, Gallis HE, Scherf J, Eitan A, Wagner HD. Continuous monitoring of the fragmentation phenomenon in single fiber composite-materials. Polym Compos 1991;12(6): 436–46.
[26] Ahlstrom C, Gerard JF. The adhesion of elastomer-coated glass-fibers to an epoxy matrix. 1. The effect of the surface treatments on the tensile-strength of the glass-fibers. Polym Compos 1995;16(4):305–12.
[27] Coleman BD. On the strength of classical fibers and fiber bundles. J Mech Phys Solids 1958;7:60–70.
[28] Weibull W. A statistical distribution function of wide applicability. J Appl Mech 1951;18(3):293–7.
[29] Davis AK. Influence of surface treatment and humidity on strength of E-glass fiber bundles. Masters Thesis, Dept. Theoretical and Applied Mechanics, University of Illinois at Urbana-Champaign; 1999.
[30] Scholze H. Glass–water interactions. J Non-Cryst Solids 1988;102(1–3):1–10.
[31] Wang Z, Xia YM. Experimental evaluation of the strength distribution of fibers under high strain rates by bimodal Weibull distribution. Compos Sci Technol 1997;57(12):1599–607.